

Boundary-corrected four-body continuum-intermediate-state method for charge exchange between hydrogenlike projectiles and atoms

Nenad Milojević,¹ Ivan Mančev,¹ and Dževad Belkić^{2,3}

¹*Department of Physics, Faculty of Sciences and Mathematics, University of Niš, P.O. Box 224, 18000 Niš, Serbia*

²*Department of Oncology-Pathology, Nobel Medical Institute, Karolinska Institute, P.O. Box 260, 171 76 Stockholm, Sweden*

³*Radiation Physics & Nuclear Medicine, Karolinska University Hospital, 171 76 Stockholm, Sweden*

(Received 1 April 2017; revised manuscript received 15 July 2017; published 18 September 2017)

Single-electron capture from one-electron and multielectron atoms colliding with hydrogenlike projectiles at intermediate and high incident energies is examined by using the post version of the boundary-corrected four-body continuum-intermediate-state (BCIS-4B) method. This method satisfies the correct boundary conditions in the entrance and exit channels. In the entrance configuration, the BCIS-4B method takes into account the ionization channel through the electronic continuum intermediate states described by the full Coulomb wave function centered on the screened nuclear charge of the projectile. The presented analytical calculation yields the transition amplitude in terms of an efficiently computed two-dimensional numerical quadrature over real variables. Total cross sections are computed for electron capture in the $\text{He}^+ - \text{H}$, $\text{He}^+ - \text{He}$, and $\text{Li}^{2+} - \text{He}$ collisions at intermediate and high impact energies. Also, differential cross sections are obtained for the $\text{He}^+ - \text{He}$ collisions. The present results from the BCIS-4B method are found to be in very good agreement with the available experimental data on differential and total cross sections.

DOI: [10.1103/PhysRevA.96.032709](https://doi.org/10.1103/PhysRevA.96.032709)

I. INTRODUCTION

Single-electron capture from one- and multielectron targets colliding with hydrogenlike projectiles has attracted a great deal of attention for decades [1–23]. In addition to the necessity of a clear understanding of fundamental collision dynamics of many-electron collision systems, detailed cross sections for these high-energy collisions are also needed in some other research fields. These include collisional interactions of energetic ion beams (often highly charged) with a neutralizer gas, with plasma in fusion experiments, with residual neutral gas in an accelerator storage ring, or with tissue in hadron therapy [6,7]. Such multiply charged ions are also encountered in astrophysics as, e.g., solar wind ions that undergo excitation, deexcitation, charge exchange, and ionization during their fast collisions with atomic systems from interstellar media.

Charge-transfer cross sections for collisions involving dressed projectiles (those bearing electrons) have been extensively studied using theories for the underlying three-body [24–35] and four-body problems [36–44], as reviewed in Refs. [1–7]. In the three-body methods, the given projectile is treated as a rigid core ion due to screening by the passive electron in the incident atomic system. With the assumption of a rigid core of the projectile ion, it is obvious that the interaction of the projectile ion with the target nucleus should be Coulombic. Some of these three-body models show satisfactory agreement with experimental data, but their basic drawback is that they completely neglect dynamic (i.e., collisional) electron-electron correlations.

The present work is a theoretical investigation of single-electron capture from one- and multielectron atoms colliding with hydrogenlike projectiles at intermediate and high incident energies. We will employ the four-body boundary-corrected continuum-intermediate-state (BCIS-4B) method. As in the general theory from Ref. [1], in the present examination of single charge exchange, the many-electron target has been

treated by way of a model with one active electron, which is to be transferred to the projectile. The other noncaptured target electrons are considered as passive and occupying the same orbitals in the initial and final states. Their role is merely to screen the target nuclear charge. The projectile electron has also been treated as active in the exactly known hydrogenlike system. The net result of this atomic model for the target is a reduction of a difficult many-particle problem to its more manageable four-body counterpart.

The BCIS-4B approximation is an adaptation of the same method introduced in Ref. [45] for double-electron capture in collisions of fast nuclei with heliumlike atomic systems. This is a fully-quantum-mechanical four-body method with a strict preservation of the correct boundary conditions in both collisional channels according to the principles of quantum scattering theory [1–5,46,47]. The matter of the correct Coulomb boundary conditions is equivalent to the concept of asymptotic convergence [47].

The post form of the BCIS-4B method is a hybrid distorted-wave model, which exactly coincides with the four-body continuum distorted-wave (CDW-4B) theory in the entrance channel and with the four-body boundary-corrected first Born (CB1-4B) approximation in the exit channel. The associated perturbation potential in the post-transition amplitude of the BCIS-4B method is the same as in the pertinent CB1-4B method. Hence, the captured electron is treated in an asymmetric manner in the entrance and exit channels. In the entrance channel, the BCIS-4B method includes the ionization channel of the active target electron. Namely, prior to being captured, this electron is ionized and treated as occupying continuum states in the intermediate stage of the collision. These states are not free, i.e., undistorted in the sense of being described by a plane wave. Rather, they are described by the electronic full Coulomb wave function centered on the screened nuclear charge of the projectile. In the exit channel, the BCIS-4B method has no electronic distortion factors. Instead, just like in the CB1-4B method, the only distortion of the unperturbed

final state is the Coulomb logarithmic phase for the relative motion of heavy particles.

By comparing the BCIS-4B and CB1-4B theories, we would learn about the relative importance of these intermediate ionization electronic continua, and this is one of the main goals of the present study. A further inquiry of this paper will be an assessment of the usefulness of the BCIS-4B method in practice by comparing the obtained theoretical results with the available experimental data for single-electron transfer from one- and multielectron targets by hydrogenlike projectiles.

Atomic units will be used throughout unless otherwise stated.

II. THEORY

In the present paper, we are interested in single charge exchange in two types of scattering events, such as collisions of hydrogenlike projectiles with hydrogenlike targets and/or multielectron targets.

A. Charge exchange with hydrogenlike projectiles on hydrogenlike targets

The rearrangement collisions to be studied in this section are of the following type:

$$(Z_P, e_1)_{i_1} + (Z_T, e_2)_{i_2} \rightarrow (Z_P, e_1, e_2)_f + Z_T, \quad (1)$$

where P (T) denotes the projectile (target) nucleus. The parentheses in Eq. (1) denote the bound states, whereas the subscript i_1 (i_2) is the collective label for the set of hydrogenlike quantum numbers $\{n_1, l_1, m_1\}$ ($\{n_2, l_2, m_2\}$) and the index f refers to the quantum numbers of the final heliumlike state. The binding energies of $(Z_P, e_1)_{i_1}$, $(Z_T, e_2)_{i_2}$, and $(Z_P, e_1, e_2)_f$ are E_P , E_T , and E_f , respectively. Throughout the paper, the quantum-mechanical nonrelativistic scattering theory will be used without accounting for the spin effects. In the spin-independent formalism, the two electrons can be considered as distinguishable from each other. The position vectors of the first and second electrons (e_1 and e_2) relative to the nuclear charge of the projectile Z_P (the target Z_T) are denoted by \vec{s}_1 and \vec{s}_2 (\vec{x}_1 and \vec{x}_2), respectively. Further, let \vec{R} be the position vector of Z_P with respect to Z_T . The vector of the distance between the two active electrons (e_1 and e_2) is labeled as $\vec{r}_{12} = \vec{x}_1 - \vec{x}_2 = \vec{s}_1 - \vec{s}_2$. In the entrance channel, it is convenient to introduce \vec{r}_i as the position vector between the center of mass of $(Z_P, e_1)_{i_1}$ and the target system $(Z_T, e_2)_{i_2}$, whereas the pertinent reduced mass and momentum wave vector are $\mu_i = (M_P + 1)(M_T + 1)/M$ and \vec{k}_i , respectively, where $M = M_P + M_T + 2$. Symmetrically, in the exit channel, let \vec{r}_f be the position vector of Z_T relative to the center of mass of $(Z_P, e_1, e_2)_f$, while the associated reduced mass and momentum vector are $\mu_f = M_T(M_P + 2)/M$ and \vec{k}_f , respectively. The reduced mass μ involving the masses of the nuclei is given by $\mu = M_P M_T / (M_P + M_T)$. The position vectors $\vec{r}_{i,f}$ and $\pm \vec{R}$ are interconnected by the general exact relations $\vec{r}_i = \vec{R} + \vec{s}_1 / (M_P + 1) - \vec{x}_2 / (M_T + 1)$ and $\vec{r}_f = -\vec{R} - (\vec{s}_1 + \vec{s}_2) / (M_P + 2)$. The incident and outgoing velocities are $\vec{v}_i = \vec{k}_i / \mu_i$ and $\vec{v}_f = \vec{k}_f / \mu_f$, respectively. The respective unit vectors of the momenta and velocities are

$\hat{k}_{i,f} = \vec{k}_{i,f} / k_{i,f}$ and $\hat{v}_{i,f} = \vec{v}_{i,f} / v_{i,f}$ where the direction of the incident or impact velocity \vec{v} (with $\vec{v} \equiv \vec{v}_i$) is chosen along the Z axis as $\hat{v} = (0, 0, 1)$, where $\hat{v} = (1/v)\vec{v}$. The vector \vec{R} of the internuclear axis R is decomposed as $\vec{R} = \vec{\rho} + \vec{Z}$, where $\vec{\rho}$ is the projection of \vec{R} onto the XOY plane such that $\vec{\rho} \cdot \vec{Z} = 0$ and $\vec{\rho} \cdot \vec{v} = 0$. For (1), as well as for the other collisional processes investigated herein, we will consistently use the independent variables $\{\vec{s}_1, \vec{x}_2, \vec{r}_i\}$ and $\{\vec{s}_1, \vec{s}_2, \vec{r}_f\}$ in the entrance and exit channels, respectively. As such, the initial forms of the derived expressions for the channel Hamiltonians, scattering wave functions, perturbation potentials, and transition matrix elements will all refer to these latter independent variables.

1. Entrance channel

As stated, in the entrance channel within the post version of the BCIS-4B method for (1), the wave function of the CDW-4B method [43] is employed:

$$\begin{aligned} \chi_i^+ &= e^{i\vec{k}_i \cdot \vec{r}_i} \varphi_P(\vec{s}_1) \varphi_T(\vec{x}_2) N^+(v_P) \\ &\times {}_1F_1(i v_P, 1, i v s_2 + i \vec{v} \cdot \vec{s}_2) \mathcal{N}^+(v_i) \\ &\times {}_1F_1(-i v_i, 1, i k_i r_i - i \vec{k}_i \cdot \vec{r}_i), \end{aligned} \quad (2)$$

where $v_P = (Z_P - 1)/v$, $v_i = Z_T(Z_P - 1)/v$, $N^+(v_P) = \Gamma(1 - i v_P) e^{\pi v_P / 2}$, and $\mathcal{N}^+(v_i) = \Gamma(1 + i v_i) e^{-\pi v_i / 2}$. The symbol Γ denotes the Gamma function, whereas ${}_1F_1(a, b, z)$ stands for the regular confluent hypergeometric function. The single-electron hydrogenlike wave functions of the $(Z_P, e_1)_{i_1}$ and $(Z_T, e_2)_{i_2}$ systems are denoted by $\varphi_P(\vec{s}_1)$ and $\varphi_T(\vec{x}_2)$ with the corresponding binding energies $E_P = -Z_P^2 / (2n_1^2)$ and $E_T = -Z_T^2 / (2n_2^2)$, respectively. It can be readily verified that the distorted wave χ_i^+ satisfies the proper boundary conditions at infinitely large interparticle separations. The function $N^+(v_P) {}_1F_1(i v_P, 1, i v s_2 + i \vec{v} \cdot \vec{s}_2)$ in χ_i^+ describes intermediate ionization of the electron e_2 . This is the electronic full continuum Coulomb wave function in the attractive electrostatic field of the screened projectile nucleus charge $V_{P2} = -(Z_P - 1)/s_2$. The screened point charge $Z_P - 1$ of the projectile $(Z_P, e_1)_{i_1}$ is introduced because at infinitely large values of s_2 , the active electron e_2 from $(Z_T, e_2)_{i_2}$ cannot discern the individual constituents in the projectile $(Z_P, e_1)_{i_1}$. In other words, at $s_2 \rightarrow \infty$, the electron e_2 experiences the hydrogenlike system $(Z_P, e_1)_{i_1}$ as a point charge $Z_P - 1$.

Within the standard eikonal approximation for fast heavy-particle collisions ($k_{i,f} \gg 1$ and $M_{P,T} \gg 1$), it is permitted to replace the full Coulomb wave function $\mathcal{N}^+(v_i) {}_1F_1(-i v_i, 1, i k_i r_i - i \vec{k}_i \cdot \vec{r}_i)$ in Eq. (2) by its logarithmic phase factor in the scattering state χ_i^+ for the distortion effect arising from the relative motion of heavy particles. This maps χ_i^+ from (2) into its eikonal counterpart $\chi_{i,\text{eik}}^+$ via

$$\begin{aligned} \chi_{i,\text{eik}}^+ &= e^{i\vec{k}_i \cdot \vec{r}_i + i v_i \ln(k_i r_i - \vec{k}_i \cdot \vec{r}_i)} \varphi_P(\vec{s}_1) \varphi_T(\vec{x}_2) N^+(v_P) \\ &\times {}_1F_1(i v_P, 1, i v s_2 + i \vec{v} \cdot \vec{s}_2). \end{aligned} \quad (3)$$

It then follows that the initial eikonal scattering state $\chi_{i,\text{eik}}^+$ also satisfies the correct Coulomb boundary conditions, just like the starting distorted wave χ_i^+ from (2). It should be emphasized that imposing the proper Coulomb boundary conditions is of crucial importance [1–4, 46, 47].

2. Exit channel

The final state Φ_f^- in the exit channel is distorted even at infinite distances between the colliding aggregates due to the long-range nature of the Coulomb interaction, as demanded by the correct boundary condition. The reason for this is the presence of the asymptotic Coulomb repulsive interaction $V_f^\infty = Z_T(Z_P - 2)/r_f$ between the target nucleus and the screened projectile nuclear charge $Z_P - 2$. Here Z_P is screened by the unit charges of each of the two electrons e_1 and e_2 to become $Z_P - 2$. Thus, the perturbed entrance channel state Φ_f^- and the corresponding perturbation potential V_f are given by

$$\Phi_f^- = \varphi_f(\vec{s}_1, \vec{s}_2) e^{-i\vec{k}_f \cdot \vec{r}_f} \mathcal{N}^-(v_f) \times {}_1F_1(i\nu_f, 1, -ik_f r_f + i\vec{k}_f \cdot \vec{r}_f), \quad (4)$$

$$V_f = \frac{Z_P Z_T}{R} - \frac{Z_T(Z_P - 2)}{r_f} - \frac{Z_T}{x_1} - \frac{Z_T}{x_2}, \quad (5)$$

respectively, where $\mathcal{N}^-(v_f)$ is the Coulomb normalization constant $\mathcal{N}^-(v_f) = e^{-\pi\nu_f/2} \Gamma(1 - i\nu_f)$, with $\nu_f = Z_T(Z_P - 2)/v$. Here $\varphi_f(\vec{s}_1, \vec{s}_2)$ is the final-bound-state wave function of the heliumlike atomic system $(Z_P, e_1, e_2)_f$. The long-range distortion effects are present in Eq. (4) through the full Coulomb wave function $\mathcal{N}^-(v_f) e^{-i\vec{k}_f \cdot \vec{r}_f} {}_1F_1(i\nu_f, 1, -ik_f r_f + i\vec{k}_f \cdot \vec{r}_f)$ for the relative motion of heavy nuclei. In the mass approximation $M_P \gg 1$, the perturbation potential V_f can be simplified as follows. Using the already stated definition of \vec{r}_f , we can develop $1/r_f$ in the Taylor-series expansion around $1/R$ with the result $1/r_f = 1/R + \gamma \hat{R} \cdot (\vec{s}_1 + \vec{s}_2)/R^2 + O(\gamma^2)$, where $\gamma = 1/(M_P + 2)$. This implies that the difference $1/R - 1/r_f$ is a short-range potential, since it is of the order of γ smaller than $\hat{R} \cdot (\vec{s}_1 + \vec{s}_2)/R^2$. This Taylor-series expansion is justified by the small values of s_1 and s_2 (of the order of Bohr radius a_0), in the exit channel where the electrons $e_{1,2}$ are bound to the heliumlike system centered at the projectile nuclear charge Z_P . Thus, ignoring the terms of the order of or smaller than $1/M_P$, we have $r_f \approx R$ (as well as $\vec{r}_f \approx -\vec{R}$), so V_f can be written as

$$V_f = \frac{2Z_T}{R} - \frac{Z_T}{x_1} - \frac{Z_T}{x_2}. \quad (6)$$

The term Z_T/R in Eq. (6), despite its R -dependent form, is not related to the internuclear potential. The entire perturbation V_f from (6) is also of a short range because it behaves like $O(1/R^2)$ for $R \rightarrow \infty$. This is shown by the Taylor expansion for $1/x_1$ around $1/R$. A small value of s_1 in the exit channel justifies such a development, since $R = |\vec{x}_1 - \vec{s}_1|$. A similar statement also holds true for $1/x_2$. Thus, for large R , we have $x_j \approx R$ ($j = 1, 2$) and therefore the potentials $-Z_T/x_1$ and $-Z_T/x_2$ each possess the same asymptotic tail $-Z_T/R$ via $-Z_T/x_j \approx -Z_T/R$ ($j = 1, 2$). Hence, at $R \rightarrow \infty$, we have from (6) that $V_f \approx 2Z_T/R - 2Z_T/R + O(1/R^2) = O(1/R^2)$. Thus, V_f is a short-range potential. Similarly to Ref. [4], working with the independent variables $\{\vec{s}_1, \vec{s}_2, \vec{r}_f\}$ for the exit channel in Eq. (1), the expression for the total Hamiltonian could also include the so-called mass-polarization term $-(1/M_P)\vec{\nabla}_{s_1} \cdot \vec{\nabla}_{s_2}$. In the present study, in order to consistently apply the eikonal approximation, this

latter term has been omitted from V_f in Eq. (6) because its contribution is merely the M_P^{-1} th fraction of the yield from $Z_T(2/R - 1/x_1 - 1/x_2)$. Another way of justifying this omission by a specific test is to verify the consistency of, e.g., the total energy conservation law in the eikonal approximation. The outcome of this direct and explicit test is that the initial and final energies of the entire system in the eikonal approximation are equal to within $O(1/M_{P,T})$ irrespective of whether the mass-polarization term is included or excluded.

The correct asymptotic form of Φ_f^- as $r_f \rightarrow \infty$ can be obtained by using the Coulomb logarithmic phase factor in the scattering state for distortion effects due to the relative motion of heavy particles as

$$\Phi_{f,\text{eik}}^- = \varphi_f(\vec{s}_1, \vec{s}_2) e^{-i\vec{k}_f \cdot \vec{r}_f - i\nu_f \ln(k_f r_f - \vec{k}_f \cdot \vec{r}_f)}. \quad (7)$$

It should be noted that in the eikonal limit, the difference between the contributions from Φ_f^- and $\Phi_{f,\text{eik}}^-$ is of the order of the reciprocal of the heavy particle masses and thus negligible.

3. Post form of the transition amplitude

The post form of the transition amplitude in the BCIS-4B approximation for the process (1) is given by the matrix element

$$T_{if} = \langle \Phi_f^- | V_f | \chi_i^+ \rangle \simeq \langle \Phi_{f,\text{eik}}^- | V_f | \chi_{i,\text{eik}}^+ \rangle, \quad (8)$$

where the perturbation potential V_f is from (6). As mentioned, the BCIS-4B method is a hybrid approximation, which is the combination of the CDW-4B and CB1-4B methods in the entrance and exit channels, respectively. Hence, in the post form of the BCIS-4B transition amplitude, the CDW-4B model is utilized for the entrance channel, whereas the CB1-4B wave function and the CB1-4B perturbation potential are employed in the exit channels. In the BCIS-4B model, the proper connection between the long-range Coulomb distortion effects and the accompanying perturbation potentials is accomplished according to the well-established principles of scattering theory [2]. As evidenced in abundant applications, imposing the correct Coulomb boundary conditions in the entrance and exit channels is of key significance [3–7].

By employing the conventional eikonal approximation with dominant forward scattering ($\hat{k}_f \approx \hat{k}_i$ or $\hat{v}_f \approx \hat{v}_i \equiv \hat{v}$) together with the mass limits $M_{P,T} \gg 1$ yielding $\vec{r}_i \approx \vec{R}$ and $\vec{r}_f \approx -\vec{R}$, the product of the logarithmic Coulomb factors from the wave functions $\chi_{i,\text{eik}}^+$ and $\Phi_{f,\text{eik}}^-$ can be reduced to a single \vec{R} -dependent phase factor

$$\begin{aligned} & e^{i\nu_i \ln(k_i r_i - \vec{k}_i \cdot \vec{r}_i) + i\nu_f \ln(k_f r_f - \vec{k}_f \cdot \vec{r}_f)} \\ & \approx e^{i\nu_i \ln(\mu v R - \mu \vec{v} \cdot \vec{R}) + i\nu_f \ln(\mu v R + \mu \vec{v} \cdot \vec{R})} \\ & = (\mu \rho v)^{2i\nu_i} (vR + \vec{v} \cdot \vec{R})^{-i\xi} \\ & = (\mu \rho v)^{2i\nu_f} (vR - \vec{v} \cdot \vec{R})^{i\xi}, \end{aligned} \quad (9)$$

where $\xi = Z_T/v$. Here and throughout the constant phase factors $\mu^{2i\nu_{i,f}}$ can be left out. As has been shown in Ref. [1], the overall phase factors $(\rho v)^{2i\nu_f}$ and $(\rho v)^{2i\nu_i}$ in Eq. (9) do not contribute to the total cross section for any values of Z_P and Z_T , so they could freely be omitted from the T -matrix elements. Crucially, for charge exchange processes in heavy particle energetic collisions, it is precisely (9) that enabled

the proof in Ref. [1] that the internuclear potential $V_{PT} = Z_P Z_T / R$ gives no contribution at all to the eikonal version of the fully-quantum-mechanical exact total cross sections. Note that the multiplying term $(\rho v)^{2i\nu_f} \equiv (\rho v)^{2iZ_T(Z_P-2)/v}$ in Eq. (9) is especially convenient for computations of differential cross sections for $Z_P = 2$, i.e., with the He^+ projectiles for which $(\rho v)^{2iZ_T(Z_P-2)/v} = 1$. On the other hand, the factor $(\rho v)^{2i\nu_i} \equiv (\rho v)^{2iZ_T(Z_P-1)/v}$ in Eq. (9) is advantageous in the case of the H projectiles ($Z_P = 1$). In both cases, $Z_P = 2$ and $Z_P = 1$, the angular distributions become directly proportional to the absolute value squared $|T_{if}|^2$ of the transition amplitudes T_{if} with no need to carry out the Fourier-Bessel transform [1].

Importantly, as per (9), the distorted-wave eikonal scattering states in the entrance and exit channels (3) and (7) can equivalently be written in the following forms:

$$\chi_{i,\text{eik}}^+ = e^{i\vec{k}_i \cdot \vec{r}_i + i\nu_i \ln(\mu v R - \mu \vec{v} \cdot \vec{R})} \varphi_P(\vec{s}_1) \varphi_T(\vec{x}_2) N^+(\nu_P) \times {}_1F_1(i\nu_P, 1, i\nu s_2 + i\vec{v} \cdot \vec{s}_2), \quad (10)$$

$$\Phi_{f,\text{eik}}^- = \varphi_f(\vec{s}_1, \vec{s}_2) e^{-i\vec{k}_f \cdot \vec{r}_f - i\nu_f \ln(\mu v R + \mu \vec{v} \cdot \vec{R})}, \quad (11)$$

respectively. Consequently, in the asymptotic regions of scattering ($R \rightarrow \infty$), the correct initial and final Coulomb boundary conditions have two sets {(3) and (7)} and {(10) and (11)} of equally valid prescriptions, respectively.

The same mass approximation $M_{P,T} \gg 1$ used in $\vec{r}_{i,f} \approx \pm \vec{R}$ also implies the like approximate equalities between the corresponding volume elements, i.e., $d\vec{r}_{i,f} \approx d\vec{R}$, so the relations $d\vec{r}_i d\vec{s}_1 d\vec{x}_2 \approx d\vec{R} d\vec{s}_1 d\vec{x}_2$ and $d\vec{r}_f d\vec{s}_1 d\vec{s}_2 \approx d\vec{R} d\vec{s}_1 d\vec{s}_2$ can be employed in the defining nine-dimensional integrals from the prior and post form of the eikonal transition amplitude, respectively. This in turn corroborates the so-called generalized nonorthogonal coordinates $\{\vec{s}_1, \vec{x}_2, \vec{R}\}$ and $\{\vec{s}_1, \vec{s}_2, \vec{R}\}$ treated from the onset as the independent variables [48] in the entrance and exit channels instead of their counterparts $\{\vec{s}_1, \vec{x}_2, \vec{r}_i\}$ and $\{\vec{s}_1, \vec{s}_2, \vec{r}_f\}$, respectively. Had we started, e.g., with the set $\{\vec{s}_1, \vec{s}_2, \vec{R}\}$ for the independent variables in the exit channel of (1), then besides the mentioned mass-polarization term, the perturbation potential V_f would contain an additional contribution due to the mixed gradient operators, $(1/M_P) \vec{\nabla}_R \cdot (\vec{\nabla}_{s_1} + \vec{\nabla}_{s_2})$. However, because of the multiplicative infinitesimally small coefficient $1/M_P \ll 1$, these latter mixed directional derivatives can also be neglected from V_f on the same ground, as done with the mass-polarization term. The correctness of such a procedure was confirmed by an explicit calculation showing that retention of $(1/M_P) \vec{\nabla}_R \cdot (\vec{\nabla}_{s_1} + \vec{\nabla}_{s_2})$ would yield a correction of the order $O(1/M_P)$ in the eikonal form of the total energy conservation in the exit channel, as was the case with the mass-polarization term. This is in full harmony with the usual mass approximation under the eikonal hypothesis, which consistently ignores every term of the order of or smaller than $1/M_P$ or $1/M_T$. It is tempting to claim that there is an unphysical situation due to a potential ambiguity in having the exit channel Hamiltonian (and hence the final perturbation potential V_f) in two different forms for the independent variables $\{\vec{s}_1, \vec{s}_2, \vec{r}_f\}$ and $\{\vec{s}_1, \vec{s}_2, \vec{R}\}$. Indeed, it would be unacceptable if two such forms were to produce different numerical results for cross sections or for any other observables. However, in the present context, the stated claim

would be misleading because both the Hamiltonians and the perturbation interactions in the exit channel in fact generate the same eikonal dynamics, accurate to within $O(1/M_P)$. This is the case for the coordinate origins placed on either M_P or μ_f , i.e., on the mass of the scattered projectile or on the reduced mass for the center of mass of the $T + (P, 2e)$ system. Here it is pertinent to recall that also within the close-coupling method, Bransden and McDowell [49] have claimed that there is a possible ambiguity in the Hamiltonian caused by switching from one set of Jacobi's coordinates to another. However, this ambiguity does not exist either, as has been shown by Belyaev *et al.* [50], with reference to the coupling operators in terms of both single and double directional derivatives (the latter being a second-order differentiation involving the mixed position vector variables for the light and heavy particles).

With this standard setting [1], the post form of the eikonal transition amplitude in the BCIS-4B method for process (1) can be written as

$$T_{if}(\vec{\eta}) = N^+(\nu_P) \iiint d\vec{s}_1 d\vec{s}_2 d\vec{R} \varphi_P(\vec{s}_1) \varphi_T(\vec{x}_2) \times \left(\frac{2Z_T}{R} - \frac{Z_T}{x_1} - \frac{Z_T}{x_2} \right) \varphi_f^*(\vec{s}_1, \vec{s}_2) e^{i\vec{\beta} \cdot \vec{R} - i\vec{v} \cdot \vec{s}_2} \times {}_1F_1(i\nu_P, 1, i\nu s_2 + i\vec{v} \cdot \vec{s}_2) (vR - \vec{v} \cdot \vec{R})^{i\xi}, \quad (12)$$

$$\vec{k}_i \cdot \vec{r}_i + \vec{k}_f \cdot \vec{r}_f = \vec{\beta} \cdot \vec{R} - \vec{v} \cdot \vec{s}_2, \quad (13)$$

where the phase $\mu^{2i\nu_f}$ is ignored. Here the vector $\vec{\beta}$ is introduced as one of the momentum transfers in the form $\vec{\beta} = -\vec{\eta} - (v/2 + \Delta E/v)\vec{v}$, where $\Delta E = E_i - E_f$ and $E_i = E_P + E_T$. The transverse component of the change in the relative linear momentum of a heavy particle is denoted by $\vec{\eta} = (\eta \cos \phi_\eta, \eta \sin \phi_\eta, 0)$, where $\vec{\eta} \cdot \vec{v} = 0$. Note that the eikonal relations $\vec{r}_{i,f} \approx \pm \vec{R}$ are used only in the arguments $\pm k_{i,f} r_{i,f} \mp \vec{k}_{i,f} \cdot \vec{r}_{i,f}$ of the confluent hypergeometric functions ${}_1F_1(\mp i\nu_{i,f}, 1, \pm i k_{i,f} r_{i,f} \mp i\vec{k}_{i,f} \cdot \vec{r}_{i,f})$ of the relative motion of heavy particles and not in the corresponding plane waves $\exp(\pm i\vec{k}_{i,f} \cdot \vec{r}_{i,f})$ from the associated full Coulomb wave functions $\mathcal{N}^\pm(\nu_{i,f}) e^{\pm i\vec{k}_{i,f} \cdot \vec{r}_{i,f}} {}_1F_1(\mp i\nu_{i,f}, 1, \pm i k_{i,f} r_{i,f} \mp i\vec{k}_{i,f} \cdot \vec{r}_{i,f})$. This is very important and it is done to fully preserve the so-called electron translation factor in the combined exponential $\exp(i\vec{k}_i \cdot \vec{r}_i + i\vec{k}_f \cdot \vec{r}_f)$ where, for predominant forward scattering of heavy particles, it follows that $\exp(i\vec{k}_i \cdot \vec{r}_i + i\vec{k}_f \cdot \vec{r}_f) \approx \exp(i\vec{\beta} \cdot \vec{R} - i\vec{v} \cdot \vec{s}_2)$, as per (13).

The post form of the transition amplitude $T_{if}(\vec{\eta})$ from (12) can be interpreted in the following way. In the entrance channel, collisions between the projectile $(Z_P, e_1)_{i_1}$ and the target nucleus Z_T accumulate the Coulombic phase factor $\exp[(i/v)Z_T(Z_P - 1) \ln(vR - \vec{v} \cdot \vec{R})]$. At the same time, the interaction of $(Z_P, e_1)_{i_1}$ with the target leads to single ionization of the active target electron e_2 in the experimentally inaccessible intermediate stage of collision. The ionized electron propagates in the Coulomb field of charge $Z_P - 1$ of the projectile ion in a particular direction with the momentum $\vec{k} = \vec{v}$. Next, capture of the electron occurs from these intermediate ionizing states (capture from the continuum) because the electron is traveling together with the screened

projectile in the same direction and the attractive Coulomb interaction between $Z_P - 1$ and e_2 is sufficient to bind them together into the heliumlike atomic system $(Z_P, e_1, e_2)_f$. Thus, in the post form of the BCIS-4B method, the continuum intermediate states refer to the continuum of the electron e_2 (to be captured), as described by the full Coulomb wave function centered on the projectile ion point charge $Z_P - 1$. Overall, in the entrance channel, the electron to be transferred is described as being simultaneously subjected to two Coulomb centers, the target and the screened projectile nuclei, which produce the bound and continuum states, respectively. As a result, the product of these two states is used as the main part of the total distorted-wave scattering state, according to the BCIS-4B method (the same also applies to the CDW-4B method, which coincides with the BCIS-4B method for the initial scattering state). On the other hand, in the exit channel, the newly formed atomic system $(Z_P, e_1, e_2)_f$ interacts with the target nucleus and accumulates the Coulombic phase factor $\exp[(-i/v)Z_T(Z_P - 2)\ln(vR + \vec{v} \cdot \vec{R})]$. Here the continuum intermediate states of the active electron are ignored altogether, as in the CB1-4B method.

Notice that the CB1-4B method can formally be obtained from (12), first through the replacement of the confluent hypergeometric function $N^+(\nu_P)_1 F_1(i\nu_P, 1, i\nu s_2 + i\vec{v} \cdot \vec{s}_2)$ by its asymptotic form $\exp[-i\nu_P \ln(\nu s_2 + \vec{v} \cdot \vec{s}_2)]$. Second, the asymptotic equality $\exp[-i\nu_P \ln(\nu s_2 + \vec{v} \cdot \vec{s}_2)] \approx \exp[-i\nu_P \ln(\nu R + \vec{v} \cdot \vec{R})]$ is employed, which is justified at large values of the internuclear distance ($R \rightarrow \infty$) at which we have $\vec{s}_2 \approx \vec{R}$.

4. Analytical calculation of the transition amplitude

In the present work, we use the general factorized form for the bound state of the heliumlike atomic system $(Z_P, e_1, e_2)_{1s^2}$ as $\varphi_f(\vec{s}_1, \vec{s}_2) = \sum_{k,l} \varphi_{\alpha k}(\vec{s}_1) \varphi_{\alpha l}(\vec{s}_2)$, where $\varphi_{\alpha j}(\vec{r}) = N_{\alpha j} \exp(-\alpha_j r)$, with $N_{\alpha j} = a_j \sqrt{N}$ ($j = k, l$) and N the normalization constant. The values of the summation indices k and l , as well as the variationally determined parameters α_j and a_j , depend upon a concrete choice for the wave function. For the confluent hypergeometric function ${}_1F_1(i\nu_P, 1, i\nu s_2 + i\vec{v} \cdot \vec{s}_2)$ in Eq. (12), we employ the integral representation

$${}_1F_1(i\nu_P, 1, i\nu s_2 + i\vec{v} \cdot \vec{s}_2) = \frac{1}{\Gamma(i\nu_P)\Gamma(1-i\nu_P)} \int_0^1 d\tau \tau^{i\nu_P-1} (1-\tau)^{-i\nu_P} e^{i(\nu s_2 + \vec{v} \cdot \vec{s}_2)\tau}, \quad (14)$$

where an infinitesimally small negative imaginary part $-i\epsilon$ ($\epsilon > 0$) is assumed to be implicitly added to the Sommerfeld parameter ν_P via $\nu_P \rightarrow \nu_P - i\epsilon$ in order to secure the convergence of the integral. Upon carrying out the calculation, the limit $\epsilon \rightarrow 0^+$ is taken, where the plus superscript indicates that ϵ tends to zero through positive numbers. Then we can cast the transition amplitude into the following form:

$$T_{if} = \mathcal{M} \int_0^1 d\tau \tau^{i\nu_P-1} (1-\tau)^{-i\nu_P} \mathcal{S}_{if}(\tau), \quad \mathcal{M} = N^+(\nu_P)/[\Gamma(i\nu_P)\Gamma(1-i\nu_P)], \quad (15)$$

$$\mathcal{S}_{if}(\tau) = \sum_{k,l} N_{\alpha k} N_{\alpha l} \int d\vec{R} e^{i\vec{\beta} \cdot \vec{R}} (vR - \vec{v} \cdot \vec{R})^{i\xi} \mathcal{T}(\vec{R}), \quad (16)$$

$$\begin{aligned} \mathcal{T}(\vec{R}) &= Z_T \iint d\vec{s}_1 d\vec{s}_2 \varphi_P(\vec{s}_1) \varphi_T(\vec{s}_2) \\ &\times \left(\frac{2}{R} - \frac{1}{x_1} - \frac{1}{x_2} \right) e^{-i\vec{v} \cdot \vec{s}_2 - \alpha_k s_1 - \alpha_l s_2 + i(\nu s_2 + \vec{v} \cdot \vec{s}_2)\tau} \\ &= Z_T \left[\frac{2}{R} W_R^{(k,l)} - W_{x_1}^{(k,l)} - W_{x_2}^{(k,l)} \right], \\ W_R^{(k,l)} &= \mathcal{A}_k \mathcal{C}_l, \quad W_{x_1}^{(k,l)} = \mathcal{B}_k \mathcal{C}_l, \quad W_{x_2}^{(k,l)} = \mathcal{A}_k \mathcal{D}_l. \end{aligned} \quad (17)$$

The quantities $\mathcal{A}_k = \int d\vec{s}_1 \varphi_P(\vec{s}_1) e^{-\alpha_k s_1}$ and $\mathcal{B}_k = \int d\vec{s}_1 \varphi_P(\vec{s}_1) e^{-\alpha_k s_1} / x_1$ can be analytically calculated, and when the wave function $\varphi_P(\vec{s}_1)$ describes the ground state, the results are

$$\begin{aligned} \mathcal{A}_k &= 8 \frac{\sqrt{\pi} Z_P^3}{(Z_P + \alpha_k)^3}, \\ \mathcal{B}_k &= 4 \frac{\sqrt{\pi} Z_P^3}{\lambda_k^2} \left[\frac{2}{\lambda_k R} - e^{-\lambda_k R} \left(1 + \frac{2}{\lambda_k R} \right) \right], \end{aligned} \quad (18)$$

where $\lambda_k = Z_P + \alpha_k$. Using the Fourier transform of $e^{-\alpha_l s_2 + i(\nu s_2 + \vec{v} \cdot \vec{s}_2)\tau}$ together with the Feynman identity, the quantity $\mathcal{C}_l = \int d\vec{s}_2 e^{-i\vec{v} \cdot \vec{s}_2 - \alpha_l s_2 + i(\nu s_2 + \vec{v} \cdot \vec{s}_2)\tau} \varphi_T(\vec{x}_2)$ can be analytically transformed to the following one-dimensional integral over a real variable t :

$$\begin{aligned} \mathcal{C}_l &= 2\mu_l \sqrt{Z_T^3 \pi} e^{-i\vec{\beta} \cdot \vec{R}} \int_0^1 dt \frac{t(1-t)}{\Delta_1^5} \\ &\times (3 + 3\Delta_1 R + \Delta_1^2 R^2) e^{-i\vec{Q}_1 \cdot \vec{R} - \Delta_1 R}, \end{aligned} \quad (19)$$

where $\mu_l = \alpha_l - i\nu\tau$, $\Delta_1^2 = v_1^2 t(1-t) + Z_T^2(1-t) + \mu_l^2 t$, $\vec{v}_1 = \vec{v}(1-\tau)$, $\vec{Q}_1 = \vec{\alpha}_1 t - \vec{\beta}(1-t)$, and $\vec{\alpha}_1 = -\vec{\beta} - \vec{v}_1$. Applying a technique similar to that for \mathcal{C}_l , the quantity $\mathcal{D}_l = \int d\vec{s}_2 \varphi_T(\vec{x}_2) e^{-i\vec{v} \cdot \vec{s}_2 - \alpha_l s_2 + i(\nu s_2 + \vec{v} \cdot \vec{s}_2)\tau} / x_2$ becomes

$$\mathcal{D}_l = 2\mu_l \sqrt{Z_T^3 \pi} e^{-i\vec{\beta} \cdot \vec{R}} \int_0^1 dt \frac{t}{\Delta_1^3} (1 + \Delta_1 R) e^{-i\vec{Q}_1 \cdot \vec{R} - \Delta_1 R}. \quad (20)$$

By employing the results from (18)–(20) and using (17), the quantity $\mathcal{S}_{if}(\tau)$ from (16) can be expressed in terms of the typical integrals $I_n = \int d\vec{R} R^{n-1} e^{-i\vec{Q}_1 \cdot \vec{R} - \lambda R} (vR - \vec{v} \cdot \vec{R})^{i\xi}$. Using the analytical results for the integrals $I_{0,1,2,3}$ that have been obtained in Ref. [51], we arrived at the following final expression for the transition amplitude T_{if} in terms of a two-dimensional integral over the real variables t and τ :

$$\begin{aligned} T_{if} &= \mathcal{K} \sum_{k,l} N_{\alpha k} N_{\alpha l} \int_0^1 d\tau \tau^{i\nu_P-1} (1-\tau)^{-i\nu_P} \frac{\mu_l}{\lambda_k^3} \\ &\times \int_0^1 dt \frac{t}{\Delta_1^3} (v_1 - i\xi \delta_1), \end{aligned} \quad (21)$$

where $\mathcal{K} = 32\pi^2 Z_T^{5/2} Z_P^{3/2} \Gamma(1+i\xi) \mathcal{M}$. The quantities v_1 and δ_1 are given in the Appendix. The remaining two-dimensional

integral in Eq. (21) is evaluated numerically and this can be done efficiently by the existing quadrature rules.

The integrand in Eq. (21) possesses integrable branch-point singularities in the part $\tau^{i\nu_P-1}(1-\tau)^{-i\nu_P}$ at $\tau = 0$ and $\tau = 1$, both of which are regularizable. Following Refs. [45,52], the customary Cauchy regularization of the whole integrand needs to be done before applying the Gauss-Legendre routine, since this quadrature rule needs to be regularized for functions with singularities. It should be noted that from the computational point of view, the BCIS-4B method is as easy as the CB1-4B approach, since in both cases the transition amplitudes are reduced to similar two-dimensional numerical quadratures.

B. Charge exchange with hydrogenlike projectiles on multielectron targets

Next we will consider single charge exchange in collisions between hydrogenlike projectiles and multielectron targets:

$$(Z_P, e_1)_{i_1} + (Z_T, e_2; \{e_3, e_4, \dots, e_{N+2}\})_{i_2} \rightarrow (Z_P, e_1, e_2)_f + (Z_T; \{e_3, e_4, \dots, e_{N+2}\}), \quad (22)$$

where the set $\{e_3, e_4, \dots, e_{N+2}\}$ denotes the N noncaptured electrons. In the case of a multielectron target, the N noncaptured electrons are considered passive such that their interactions with both active electrons e_1 and e_2 are viewed as not contributing to the capture process. We also suppose that passive electrons occupy the same orbitals before and after the collisions [1], and this is recognized as the frozen-core approximation. In such an atomic model, the passive electrons do not take part individually in the transfer of the active electron and their presence is approximately taken into account by using an effective local target potential V_T with the appropriate screening effect.

As a consequence of the outlined procedure, an explicit introduction of N passive electrons into the transition amplitude for process (22) is avoided altogether. In this way, the original many-body rearrangement collision is reduced to a purely four-body scattering problem. In the present work, we will employ the Roothan-Hartree-Fock (RHF) atomic model for the target. According to this model, the nonlocal atomic potential is approximated by an effective Coulomb interaction. This is an effective interaction V_T conceived as a pure Coulombic target potential $V_T(x_2) = -Z_T^{\text{eff}}/x_2$. Here Z_T^{eff} is the effective nuclear charge. The value of Z_T^{eff} is determined, as suggested in Ref. [1], from the relation $Z_T^{\text{eff}} = n_i(-2E_T^{\text{RHF}})^{1/2}$. The quantity E_T^{RHF} is the RHF orbital energy and n_i is the principal quantum number of the target electron to be captured. The RHF energies E_T^{RHF} are computed within the self-consistent-field method [53] and their values are known to be in close agreement with the experimentally determined binding energies. For the initial bound state of the active electron (e_2) from the multielectron target, we will use the RHF wave function given as a linear combination of the normalized Slater-type orbitals (STOs) [53] via $\psi_T^{\text{RHF}}(\vec{x}_2) = \sum_{k=1}^{N_i} C_k \chi_{n_k l_i m_i}^{(\alpha_k)}(\vec{x}_2)$, where $\chi_{n_k l_i m_i}(\vec{x}_2) = \sqrt{(2\alpha_k)^{1+2n_k}/(2n_k)!} x_2^{n_k-1} e^{-\alpha_k x_2} Y_{l_i m_i}(\hat{x}_2)$. Here C_k and α_k are the variational parameters and n_k is the orbital number. The upper summation index N_i in $\psi_T^{\text{RHF}}(\vec{x}_2)$ is the total number of STOs used in describing a given shell of the target from which capture is taking place. In Ref. [53],

the values of N_i for many atomic systems are listed along with all the other relevant parameters.

As stated, a direct consequence of the outlined simplifications is a reduction of the multielectron process (22) to a four-body problem of the general type:

$$(Z_P, e_1) + (Z_T^{\text{eff}}, e_2) \rightarrow (Z_P, e_1, e_2) + Z_T^{\text{eff}}. \quad (23)$$

In the present paper, as an illustration of collisions of the kind (22), a helium atom is considered as the target. The quoted RHF wave function from Ref. [53], specifically for $\text{He}(^1S)$, is $\varphi_T^{\text{RHF}}(\vec{x}_2) = (1/\sqrt{\pi}) \sum_{i=1}^5 C_i e^{-\zeta_i x_2}$, where $C_1 = 1.296\,27$, $C_2 = 0.818\,831$, $C_3 = 0.376\,271$, $C_4 = -0.165\,751$, $C_5 = 0.051\,483$, $\zeta_1 = 1.417\,14$, $\zeta_2 = 2.376\,82$, $\zeta_3 = 4.396\,28$, $\zeta_4 = 6.526\,99$, $\zeta_5 = 7.942\,52$, $E_T^{\text{RHF}} = -0.917\,95$, and $Z_T^{\text{eff}} = 1.354\,954$.

Expressions for the total and differential cross sections

In the case of arbitrary values of the projectile and target nuclear charges Z_P and Z_T , respectively, the general expression for the total cross sections is given by

$$Q(\pi a_0^2) = \frac{1}{2\pi^2 v^2} \int_0^\infty d\eta \eta |T_{if}(\vec{\eta})|^2. \quad (24)$$

In the computations of the total cross sections from (24), three-dimensional quadratures are performed numerically. Throughout the computations, the Gauss-Legendre quadrature rule is employed for the numerical integration over τ and t according to (21). The remaining integration over η is also carried out by means of the Gauss-Legendre routine, after performing the change of variable $\eta = \sqrt{2(1+z)/(1-z)}$, where $z \in [-1, +1]$, as suggested in Ref. [54]. This latter change of variable is important, since it concentrates the integration points near the forward cone, which provides the main contribution to the total cross section. The branch-point singularity is only apparent at $z = 1$, since it disappears altogether after analytical scaling of the integrand.

In addition to the total cross sections, we are presently interested in the computation of the angular distributions of the projectiles scattered into the solid angle $\Omega = \{\theta, \phi\}$. Comparisons of the theoretical and experimental differential cross sections will be made for single-electron capture in the He^+ -He collisions. In this case we have $Z_P = 2$, so the remaining phase factor $(\rho v)^{2i\nu_f}$ from (9) becomes unity, $(\rho v)^{2i\nu_f} \equiv (\rho v)^{2iZ_T(Z_P-2)/v} = 1$. Therefore, for such collisions, the angular distributions can be computed by simply squaring the absolute value of the transition amplitude with no recourse to the Fourier-Bessel transform [1]. Then the formula for the differential cross sections in the center-of-mass system becomes

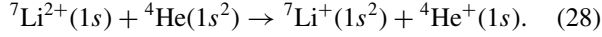
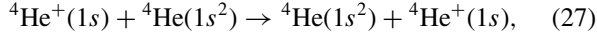
$$\frac{dQ}{d\Omega}(a_0^2/\text{sr}) = \frac{\mu^2}{4\pi^2} |T_{if}(\vec{\eta})|^2. \quad (25)$$

The scattering angle θ in $\Omega = \{\theta, \phi\}$ is defined by reference to η through $\eta = 2\mu v \sin(\theta/2)$.

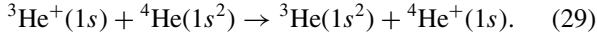
III. RESULTS OF NUMERICAL COMPUTATIONS

Using (24), numerical computations of the total cross sections are presently carried out for the following charge

exchange processes:



On the other hand, by employing (25), computations of the differential cross sections are performed for the electron transfer process:



Note that among all these listed processes, only (28) exhibits both charged scattering aggregates (in the exit channel). In the other processes (26), (27), and (29), only one scattering particle is charged. Nevertheless, the presented theory is general and as such applicable to all the relevant processes irrespective of whether the scattering particles are charged or not. This is because whenever the electronic Coulomb wave functions are used to describe the distortions of the unperturbed channel states, this must be balanced out by the introduction of the corresponding Coulomb asymptotic phases for the relative motions of heavy nuclei in order to preserve the correct Coulomb boundary conditions. In the BCIS-4B method, at least one such balancing Coulomb phase survives. This is the case with all the above processes (26)–(29). This is the reason for imposing the correct boundary conditions even when only one of the scattering particles is charged, as in Eqs. (26), (27), and (29). Recall that Cheshire [46] introduced the correct Coulomb boundary conditions within the three-body continuum distorted-wave method for the prototypal charge exchange in the $\text{H}^+ + \text{H} \rightarrow \text{H} + \text{H}^+$ collisions, even though no Coulomb interaction is present between protons and neutral hydrogen atoms in the entrance and exit channels.

A. Total cross sections: Theories versus experiments

The eikonal approximation (13) has been widely used in the framework of the different three- and four-body methods [1,3,4]. Justification of such an approximation can be demonstrated, e.g., in the case of single capture in the p -He and He^{2+} -He collisions by means of the CB1-4B method [55] and the four-body Coulomb-Born distorted-wave (CBDW-4B) method [56,57], which also obeys the correct boundary conditions. There are two differences between the CBDW-4B and CB1-4B methods. One is that the former and the latter employ the full Coulomb wave functions and the corresponding Coulomb logarithmic phases, respectively, for the relative motion of heavy particles. The other is that the CB1-4B method uses the forward-angle simplification (13), whereas the CBDW-4B method does not. In other words, the CB1-4B method is the eikonal version of the fully-quantum-mechanical CBDW-4B method. Of course, in the post-transition amplitude, both the CBDW-4B and CB1-4B methods have the same perturbation potential V_f . Detailed comparisons between the CBDW-3B and CB1-3B approximation for processes with three-body charge exchange have been made in Ref. [58] with the outcome of having virtually the same cross sections in both methods. Further, and this is also important, it was specifically shown in Ref. [58] that

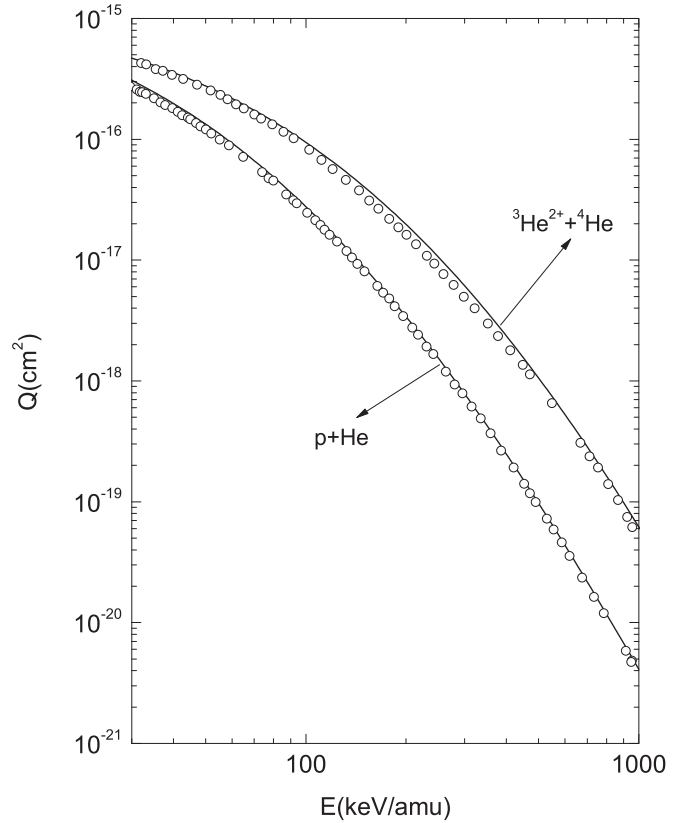


FIG. 1. Theoretical total cross sections Q (cm^2) for single charge exchange as a function of the laboratory incident energy E (keV/amu). The curves show the results obtained by means of the CB1-4B method [55] for the process $\text{H}^+ + \text{He}(1s^2) \rightarrow \text{H}(1s) + \text{He}^+(1s)$ (lower curve) and the process $\text{He}^{2+} + \text{He}(1s^2) \rightarrow \text{He}^+(1s) + \text{He}^+(1s)$ (upper curve). The open circles represent the theoretical results of the CBDW-4B method [56,57] for the mentioned processes. All the computations were carried out using the same one-parameter wave function of Hylleraas for the helium target, $\text{He}(1s^2)$.

the cross sections in the CBDW method at intermediate and high impact energies remained practically unaltered by the mass approximations for the position vectors of heavy nuclei, such as $\vec{r}_i \approx \vec{R}$ and $\vec{r}_f \approx -\vec{R}$, within the arguments of the confluent hypergeometric functions for the relative motion of heavy particles.

Presently, a comparison of the total cross sections for single-electron capture predicted by the CBDW-4B [56,57] and the CB1-4B [55] methods is made in Fig. 1 for the p -He and He^{2+} -He collisions at impact energies between 30 and 1000 keV/amu . As can be seen from this figure, both methods give nearly the same results. As a further test, which is extended to higher impact energies than those in Fig. 1, we have carried out another computation of the cross sections. Namely, we use the fully-quantum-mechanical boundary-corrected continuum intermediate state (QBCIS) method without the eikonal hypothesis. First, as opposed to the BCIS-4B method, the forward-angle simplification (13), as a part of the eikonal approximation, is not employed in the QBCIS-4B method. Second, regarding the relative motions of heavy particles, the QBCIS-4B method uses the full Coulomb

wave functions, as per (2) and (4) in the initial and final scattering states, respectively, in lieu of the corresponding logarithmic Coulomb phases of the BCIS-4B method. Thus, as far as the eikonal approximation is concerned, especially for the relative motions of heavy particles, the difference between the pair of the second-order methods (QBCIS-4B and BCIS-4B) is precisely the same as the difference between the corresponding first-order methods (CBDW-4B and CB1-4B). To compare the QBCIS-4B and BCIS-4B methods, we consider single charge exchange in the ${}^4\text{He}^+(1s) + \text{H}(1s)$ collisions at three impact energies of 5, 7.5, and 12.5 MeV/amu. With this goal, it is sufficient for the purpose of this second test to employ only the term $-Z_T/x_1$ in the perturbation potential V_f from (6). The ensuing results of the QBCIS-4B and BCIS-4B methods are shown in Fig. 2, where they can be seen to be in perfect agreement. Taken together, Figs. 1 and 2 for high-energy ($k_{i,f} \gg 1$) heavy-particle ($M_{P,T} \gg 1$) collisions testify to the proper use of the standard eikonal approximation in the BCIS-4B (present computation) and also, retrospectively, in the CB1-4B method [55]. This in turn confirms the validity of all the employed relations in the BCIS-4B and CB1-4B methods via $\hat{v}_f \approx \hat{v}_i$ and $\vec{r}_{i,f} \approx \pm \vec{R}$, as well as $\mathcal{N}^\pm(v_{i,f}) {}_1F_1(\mp i v_{i,f}, 1, \pm i k_{i,f} r_{i,f} \mp i \vec{k}_{i,f} \cdot \vec{r}_{i,f}) \approx (\pm k_{i,f} r_{i,f} \mp \vec{k}_{i,f} \cdot \vec{r}_{i,f})^{\pm i v_{i,f}} \approx (\pm \mu v R - \mu \vec{v} \cdot \vec{R})^{\pm i v_{i,f}}$.

Next we proceed to illustrate the BCIS-4B method for the processes listed in Eqs. (26)–(28). First, we will consider the asymmetric process (26). This collision between the helium ions (He^+) and the hydrogen atoms (H) is one of the simplest and most basic collision problems involving two composite atomic systems. The wave functions for these systems in the entrance channel are known exactly, whereas the state of the helium atom in the exit channel is described by means of the configuration-interaction wave function ($1s1s'$) from Ref. [59] with the radial static correlations $\varphi_f(\vec{s}_1, \vec{s}_2) = (N/\pi)(e^{-\alpha_1 s_1 - \alpha_2 s_2} + e^{-\alpha_2 s_1 - \alpha_1 s_2})$, where $N^{-2} = 2[(\alpha_1 \alpha_2)^{-3} + (\alpha_1/2 + \alpha_2/2)^{-6}]$. The following variationally determined parameters are used for $\text{He}(1s^2)$: $\alpha_1 = 2.183\,171$ and $\alpha_2 = 1.188\,530$. The ground-state energy of the He atom for this wave function [59] is $E_f = -2.875\,661\,4$. The use of this simple representation of the He atom (with about 90% of radial correlations) is justified and should give a reasonable description of the final ground-state for this particular process. Previously, this wave function from Ref. [59] has successfully been used in many studies (see, e.g., the reviews [3,4]). The results of the computations of the total cross sections for this process at impact energies 50–5000 keV are displayed in Fig. 3(c). The explicit computations of the total cross sections are carried out only for capture into the final ground state $1s^2$. In Fig. 3(c), we have compared the present cross sections from the BCIS-4B approximation with the corresponding results obtained by means of the CB1-4B [41] and CDW-4B [43] methods, as well as with a number of experimental findings [15,19,21]. All the computations presented in this figure refer to the post form. The cross sections of the BCIS-4B approximation are observed to be in good agreement with measurements at impact energies $E \geq 100$ keV. Moreover, all three computations yield quite similar results at intermediate and higher impact energies. As expected, at lower impact energies, considerable differences exist among the BCIS-4B, CB1-4B, and CDW-4B approximations.

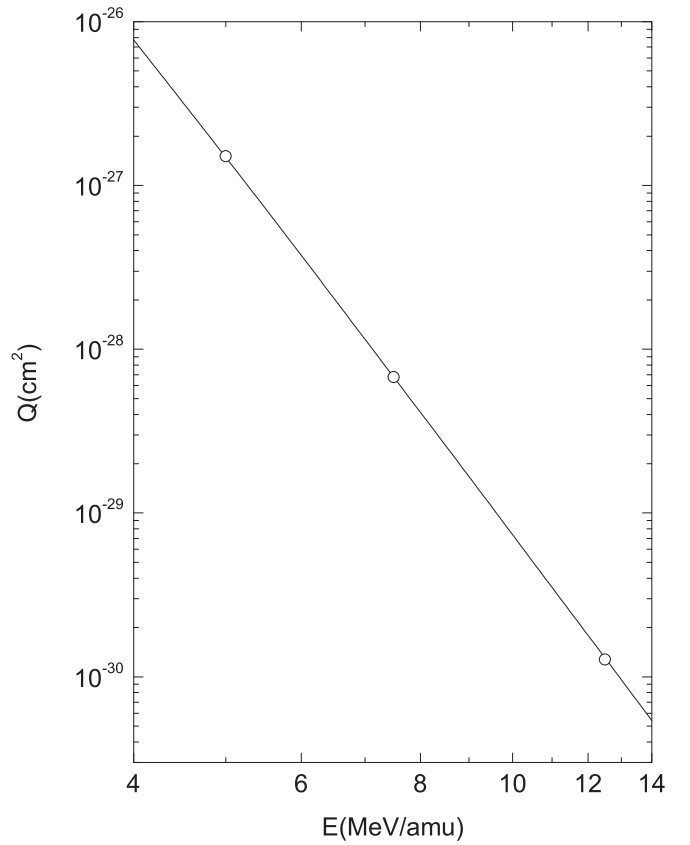


FIG. 2. Theoretical total cross sections Q (cm²) for single charge exchange in the ${}^4\text{He}^+(1s) + \text{H}(1s)$ collisions as a function of the laboratory incident energy. The shown cross sections include only the term $-Z_T/x_1$ in the perturbation potential V_f from (6). The open circles represent the results from the QBCIS-4B method, whereas the solid line shows results from the BCIS-4B method. All the computations were performed using the two-parameter wave function of Silverman *et al.* [59] for the helium atom in its ground state, $\text{He}(1s^2)$. The BCIS-4B method is the eikonal version of the QBCIS-4B method, which is the fully quantum-mechanical four-body boundary-corrected continuum-intermediate-state approximation. For the relative motion of heavy particles in the initial and final states, the QBCIS-4B and BCIS-4B methods utilize the full Coulomb wave functions and the associated logarithmic phases, respectively. The other difference is that the BCIS-4B method employs the forward-angle simplification of the eikonal type in the arguments of plane waves as per (13), whereas the QBCIS-4B method uses directly $\vec{k}_i \cdot \vec{r}_i + \vec{k}_f \cdot \vec{r}_f$ without resorting to the simplification (13).

The results from the BCIS-4B approximation for the $\text{He}^+ - \text{He}$ collisions in the energy range from 40 to 3000 keV/amu are plotted in Fig. 3(b). A comparison between the theoretical results and numerous experimental data shown in this figure also reveals good agreement above 100 keV/amu. As anticipated with high-energy methods, all the theoretical curves (BCIS-4B, CB1-4B, and CDW-4B) displayed in this figure overestimate the experimental data at lower impact energies, especially in the case of the CDW-4B model [43].

In addition to electron capture into the ground $1s^2$ final state, which is described in the present work, several other processes can also occur. These are electron transfer to an excited state of the atomic system with the projectile nucleus, electron

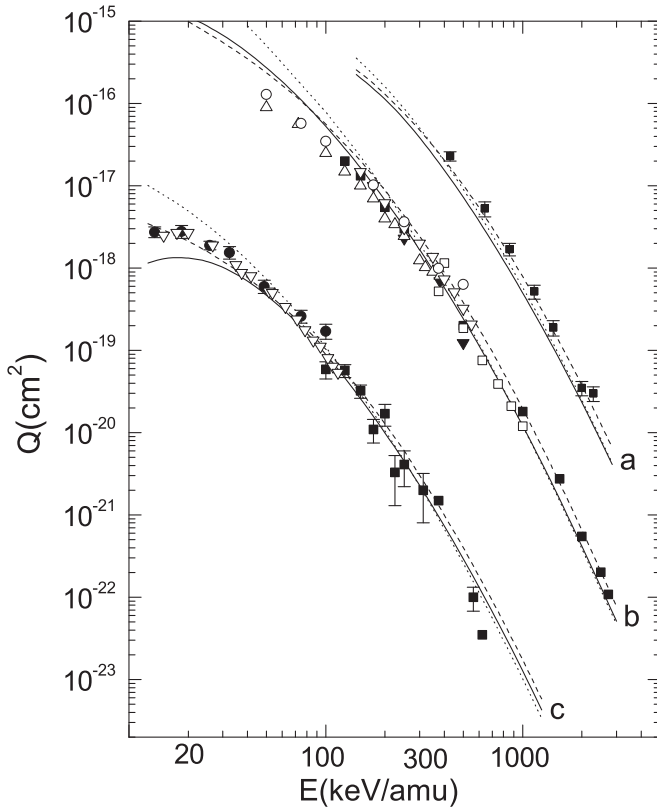


FIG. 3. Total cross sections (in cm^2) as a function of the laboratory incident energy E (keV/amu). Curves in a are for the ${}^7\text{Li}^{2+} + {}^4\text{He}^+ \rightarrow {}^7\text{Li}^+ + {}^4\text{He}^+$ collisions. All the results (theoretical and experimental) for this process are multiplied by 10. The experimental data are from [10] (■). Curves in b are for the ${}^4\text{He}^+ + {}^4\text{He} \rightarrow {}^4\text{He} + {}^4\text{He}^+$ collisions. The experimental data are from Ref. [11] (■), Ref. [16] (□), Ref. [14] (○), Ref. [13] (▽), Ref. [22] (▼), and Ref. [23] (△). Curves in c are for the ${}^4\text{He}^+ + \text{H} \rightarrow {}^4\text{He} + \text{H}^+$ collisions. All the results (theoretical and experimental) for this process are divided by 100. The experimental data are from Ref. [19] (●), Ref. [15] (■), and Ref. [21] (▽). The solid curves represent the total cross sections in the BCIS-4B method (present computation). The dotted curves display the results from the CDW-4B method [43]. The dashed curves depict the results from the CB1-4B method [41,42]. All the computations refer to the post forms and have been carried out by using the two-parameter wave function of Silverman *et al.* [59] for the $\text{Li}^+(1s^2)$ and $\text{He}(1s^2)$ in the exit channels and the RHF wave function [53] for the helium target in the entrance channels.

capture accompanied by target excitation [transfer excitation (TE)], or processes where one target electron is captured whereas the remaining target electron is ionized (transfer ionization). Schöffler *et al.* [60] measured the projectile scattering-angle dependence for various electronic final states for single-electron capture in the He^+ -He collisions at impact energies between 60 and 630 keV/amu. They investigated the ratio of different capture channels to capture into the ground state, which is usually a dominant channel. Further, formation of the singly and doubly excited states in the He^+ -He collisions was the subject of the investigations in Refs. [61,62]. Winter and Lin [63] computed cross sections for electron capture into each singly excited state of He up to $4^{1,3}D$ by the He^+ impact on He in the energy range 0.1–10 MeV using

the Jackson-Schiff-Bates-Dalgarno version of the first Born approximation [1]. They showed that the contributions to the total cross section from excited states for these collisions were 13%, 15%, and 9% at impact energies of 0.1, 1.0, and 10 MeV, respectively. The experimental data for the sum of all cross sections corresponding to the $2lnl'$ configuration in the TE process for the He^+ -He collisions have been reported in Ref. [64]. Therein, the obtained results were found to be smaller than the cross sections for all the states by about 100, 45, and 60 times at impact energies of 50, 100, and 150 keV/amu, respectively. The presently used BCIS-4B theory describes only capture to the $1s^2$ final state. Nevertheless, on the basis of the above-mentioned facts and according to a smaller contribution from the excited states by a factor of n_f^{-3} for $n_f \geq 2$ (the Oppenheimer scaling law) relative to the ground state ($n_f = 1$) [1], it is anticipated that the inclusion of electron capture into the excited states would not significantly influence the presently reported total cross sections.

The theoretical results for formation of the Li^+ ion in the Li^{2+} -He collisions at impact energies 1–20 MeV are shown in Fig. 3(a). The two-parameter wave function from Ref. [59] for the $\text{Li}^+(1s^2)$ ion in the exit channel is utilized with the variationally determined parameters $\alpha_1 = 3.294\,909$ and $\alpha_2 = 2.078\,981$ and with the associated ground-state energy $E_f = -7.248\,748$. Our total cross sections are compared with the experimental data from Ref. [10]. As can be seen from this figure, the BCIS-4B model slightly underestimates the experimental data. In Fig. 3(a), the results from the CB1-4B approximation [42] are also plotted. The BCIS-4B method provides cross sections that are smaller than the associated results of the CB1-4B approximation throughout the considered energy range. The difference between the findings of the BCIS-4B and CB1-4B methods increases as the impact energy is augmented. Thus, the difference between the results of the BCIS-4B and CB1-4B methods can be directly attributed to the importance of the full Coulomb electronic continuum intermediate states that are retained and ignored in the former and latter approximations, respectively. As can be seen in Fig. 3(a), at higher impact energies, the BCIS-4B method gives results that are similar to those from the CDW-4B method [43]. It should be recalled that in the CDW-4B method, the electronic continuum intermediate states are included in both channels through the full Coulomb waves. The presently used impact energy intervals for the processes (26)–(28) are dictated by the available experimental data. The obtained theoretical total cross sections for processes (27) and (28) are multiplied by 2 to account for the presence of two electrons in the K shell of the helium target.

B. Differential cross sections: Theories versus experiments

Next we turn our attention to differential cross sections that provide a more sensitive test for all the theoretical models. Figure 4 shows the results of the BCIS-4B method for differential cross sections in the ${}^3\text{He}^+ + {}^4\text{He}$ collisions via (29) at impact energies of 300 keV/amu (curve a) and 630 keV/amu (curve b). These theoretical findings are compared with the corresponding measured data reported in Ref. [9]. The differential cross sections from Ref. [9] have been measured with a high resolution using cold-target

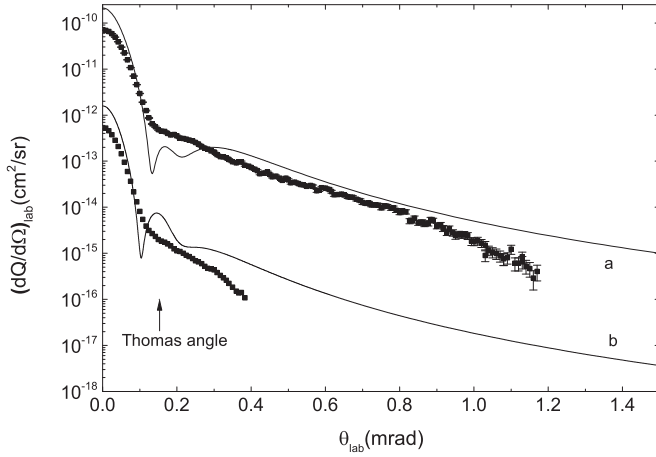


FIG. 4. The data near curve a show the differential cross sections as a function of scattering angle $\theta \equiv \theta_{\text{lab}}$ (mrad) in the laboratory frame of reference at the incident energy $E = 300$ keV/amu for single-electron capture in the ${}^3\text{He}^+ + {}^4\text{He} \rightarrow {}^3\text{He} + {}^4\text{He}^+$ collisions. The solid curve represents the theoretical results obtained by using the post form of the BCIS-4B method (present computations). The ground state of $\text{He}(1s^2)$ in the exit channel is described by means of the two-parameter wave function of Silverman *et al.* [59]. The RHF wave function for the helium target in the entrance channel has been used. The experimental data are from [9] (■). The data near curve b are the same as for curve a, except for the incident energy of $E = 630$ keV/amu. Both the theoretical and experimental results at this energy are divided by a factor of 10.

recoil ion momentum spectroscopy. At small scattering angles, associated with a dominant contribution to the total capture cross section, the transverse momentum exchange in electron transfer is mediated by the electron. However, at larger deflection angles, the scattering is dominated by momentum exchange between the nuclei. The BCIS-4B theory can be seen in Fig. 4 to be in good agreement with the experimental data [9] at small scattering angles. Nevertheless, there is a difference between the measurement and the theory at larger angles that belong to the region of the Rutherford collision for heavy aggregates. Therein, despite a proper inclusion of the Rutherford collisional effect, the BCIS-4B method still overestimates the experimental data. One of the possible reasons for this discrepancy could be the present reduction of a five-body to a four-body problem. More experimental measurements on angular distributions of scattered heavy projectiles would be welcome for further tests of high-energy methods for rearranging collisions.

The BCIS-4B approximation predicts a noticeable Thomas peak, which for the considered collision system appears at $\theta_{\text{lab}} = (1/M_P) \sin 60^\circ \simeq 0.153$ mrad. On the other hand, the experimental data [9] do not exhibit the Thomas peak, because the impact energy is not high enough to allow detection of this structure. The BCIS-4B model exhibits two interference-type dips (masked and as such unobserved by the measurement) located before and after the Thomas peak. These dips are due to partial cancellations of the repulsive and attractive potentials in the perturbation interaction V_f from (6), as well as to the interference between the full electronic Coulomb wave

function and the Coulomb logarithmic phase for the relative motion of heavy particles.

IV. CONCLUSION

Using the four-body boundary-corrected continuum-intermediate-state method, we have investigated single-electron capture from one- and multielectron targets colliding with hydrogenlike projectiles. The total scattering wave functions of the BCIS-4B approximation satisfy the correct boundary conditions in both the entrance and exit channels, according to the well-known principles of quantum scattering theory. The captured electron is treated in an asymmetric manner in the entrance and exit channels. Namely, the BCIS-4B method is a hybrid approximation, which is the combination of the four-body versions of the continuum distorted-wave method, in the entrance channel and the boundary-corrected first Born method in the exit channel. The associated perturbation potential in the post form of the transition amplitude coincides with the corresponding interaction encountered in the CB1-4B method. The BCIS-4B method accounts for the continuum intermediate states of the captured electron in the entrance channel through the use of the full Coulomb wave function centered on the screened projectile nucleus charge. We have carried out an analytical reduction of the original nine-dimensional integral for the post form of the transition amplitude to a two-dimensional real integral, which is readily amenable to efficient numerical computations.

The obtained theoretical total cross sections for the studied charge transfer processes in the $\text{He}^+ - \text{H}$, $\text{He}^+ - \text{He}$, and $\text{Li}^{2+} - \text{He}$ collisions at intermediate and high impact energies are found to be in very good agreement with the available experimental data. Comparisons are made between the results from the BCIS-4B and CB1-4B methods. The latter method ignores the continuum intermediate states of the electron and includes only the logarithmic Coulomb phase distortions due to the relative motion of heavy particles. This comparison shows that the full Coulomb electronic continuum intermediate states of the captured electron play a very important role for single-electron capture. Reduction of the total cross sections at higher impact energies is observed in the BCIS-4B method in comparison with the corresponding results of the CB1-4B method. This latter method incorporates only the direct collisional path without any double-electron scattering effects. Such a pattern can be explained by the following argument. The captured electron is intermediately found in the on-shell continuum state of the screened projectile ion with the Coulomb point charge $Z_P - 1$ prior to the actual capture. Since the electron is not staying in this continuum state in the final stage of the collision, the probability for single-electron transfer to a discrete state in the projectile Coulomb field is reduced. This reduction is more pronounced in the case of the asymmetric charge exchange in the $\text{Li}^{2+} - \text{He}$ collisions at higher impact energies.

The differential cross sections are computed for the $\text{He}^+ - \text{He}$ collisions at intermediate impact energies such as 300 and 630 keV/amu. In this five-body problem, the presently adopted atomic model accounts for the presence of the noncaptured target electron through its screening effect and describes the captured electron by means of the RHF wave function [53].

Despite such a reduction of a five-body to a four-body problem, the results obtained in the BCIS-4B method are in good agreement with the associated measured data. Both the predicted and the measured angular distributions are sharply peaked in a very narrow forward cone, where the agreement between the BCIS-4B theory and the experiment is very good. Additionally, the present theory for differential cross sections predicts another peak at the so-called critical angle. This supplementary structure is a quantum-mechanical counterpart of the Thomas peak associated with the billiard-type, classical Thomas double scattering effect. Despite the achieved high angular resolution in the measurement [9] for charge exchange in the He^+ -He collisions, the Thomas peak has not been detected. One of the reasons for this lies in the occurrence that at a relatively low incident energy, such as 630 keV/amu, the Thomas peak might be obscured by convolution of the experimentally determined angular distribution with a finite resolving power of the measuring apparatus. In the future, for a more stringent test of second-order distorted-wave theories, such as the BCIS-4B method, it would be desirable to also provide the apparatus resolution profile, along with the measured angular distributions of scattered projectiles. Such a point-spread function could advantageously be used to deconvolve the measured apparent differential cross sections. This could possibly unfold the Thomas peak in measurements even at relatively low impact energies of the order of 1000 keV/amu, at which the BCIS-4B method predicts a clear signature for double-scattering events in the presently examined charge exchange processes. Alternatively, for still better agreement between the BCIS-4B method and experiments on angular distributions, the theory could be folded with a point-spread function (whenever available) due to the measuring device, as has earlier been done in, e.g., Ref. [2].

ACKNOWLEDGMENTS

I.M. and N.M. thank the Ministry of Education, Science and Technological Development of the Republic of Serbia for support through Project No. 171020. Dž.B. appreciates support from the Research Funds of the Radiumhemmet and the Fund for Research, Development and Education of the Stockholm County Council.

APPENDIX

Quantities v_1 and δ_1 from (21) in the main text are defined as $v_1 = v_2 + v_3$ and $\delta_1 = \delta_2 + \delta_3$, where

$$v_2 = 2\mathcal{F}^{(\Delta_1)}[3p + 2(3p\Delta_1 - 1)D^{(\Delta_1)} - 2(p\Delta_1 - 1)D^{(\Delta_1)}A_\alpha^{(\Delta_1)}], \quad (\text{A1})$$

$$v_3 = 2p\mathcal{F}^{(\Delta)}\left[3 + 3(\lambda_k + 2\Delta_1)D^{(\Delta)} - \Delta_1(3\lambda_k + 2\Delta_1) \times D^{(\Delta)}\frac{A_\alpha^{(\Delta)}}{\Delta} - 2\lambda_k\Delta_1^2(D^{(\Delta)})^2\frac{A_\beta^{(\Delta)}}{\Delta}\right], \quad (\text{A2})$$

$$\delta_2 = 2\mathcal{F}^{(\Delta_1)}[2(3p\Delta_1 - 1)D^{(\Delta_1)}C^{(\Delta_1)} + 2(p\Delta_1 - 1)D^{(\Delta_1)}B_\alpha^{(\Delta_1)}], \quad (\text{A3})$$

$$\delta_3 = 2p\mathcal{F}^{(\Delta)}\left[3(\lambda_k + 2\Delta_1)D^{(\Delta)}C^{(\Delta)} + \Delta_1(3\lambda_k + 2\Delta_1) \times D^{(\Delta)}\frac{B_\alpha^{(\Delta)}}{\Delta} + 2\lambda_k\Delta_1^2(D^{(\Delta)})^2\frac{B_\beta^{(\Delta)}}{\Delta}\right], \quad (\text{A4})$$

$$p = \frac{(1-t)Z_T}{\Delta_1^2}, \quad \mathcal{F}^{(\lambda)} = \frac{[B^{(\lambda)}]^{i\xi}}{Q_1^2 + \lambda^2}, \quad (\text{A5})$$

$$B^{(\lambda)} = \frac{2(v\lambda + i\vec{Q}_1 \cdot \vec{v})}{Q_1^2 + \lambda^2},$$

$$C^{(\lambda)} = \frac{v}{\lambda B^{(\lambda)}} - 1, \quad A^{(\lambda)} = \frac{\lambda^2}{Q_1^2 + \lambda^2}, \quad D^{(\lambda)} = \frac{A^{(\lambda)}}{\lambda}, \quad (\text{A6})$$

$$\Delta = \Delta_1 + \lambda_k, \quad \lambda = \Delta \quad \text{or} \quad \Delta_1,$$

$$A_\alpha^{(\lambda)} = 1 - 4A^{(\lambda)}, \quad B_\alpha^{(\lambda)} = 1 + 2A^{(\lambda)}C_\alpha^{(\lambda)}, \quad (\text{A7})$$

$$C_\alpha^{(\lambda)} = C^{(\lambda)}[4 + (1 - i\xi)C^{(\lambda)}],$$

$$A_\beta^{(\Delta)} = 6[1 - 2A^{(\Delta)}], \quad B_\beta^{(\Delta)} = 2A^{(\Delta)}C_\beta^{(\Delta)} + 3D_\beta^{(\Delta)}, \quad (\text{A8})$$

$$D_\beta^{(\Delta)} = 2 - (1 + i\xi)C^{(\Delta)},$$

$$C_\beta^{(\Delta)} = C^{(\Delta)}\{18 + 9(1 - i\xi)C^{(\Delta)} + (1 - i\xi)(2 - i\xi)[C^{(\Delta)}]^2\}. \quad (\text{A9})$$

-
- [1] Dž. Belkić, R. Gayet, and A. Salin, *Phys. Rep.* **56**, 279 (1979).
 - [2] Dž. Belkić, *Principles of Quantum Scattering Theory* (Institute of Physics, Bristol, 2004).
 - [3] Dž. Belkić, *Quantum Theory of High-Energy Ion-Atom Collisions* (Taylor & Francis, Oxford, 2008).
 - [4] Dž. Belkić, I. Mančev, and J. Hanssen, *Rev. Mod. Phys.* **80**, 249 (2008).
 - [5] Dž. Belkić, *J. Math. Chem.* **47**, 1420 (2010).
 - [6] *Fast Ion-Atom and Ion-Molecule Collisions*, edited by Dž. Belkić (World Scientific, Singapore, 2013).
 - [7] *Theory of Heavy Ion Collision Physics in Hadron Therapy*, edited by Dž. Belkić (Elsevier, Amsterdam, 2014).
 - [8] D. L. Guo, X. Ma, R. T. Zhang, S. F. Zhang, X. L. Zhu, W. T. Feng, Y. Gao, B. Hai, M. Zhang, H. B. Wang, and Z. K. Huang, *Phys. Rev. A* **95**, 012707 (2017).
 - [9] M. S. Schöffler, J. Titze, L. P. H. Schmidt, T. Jahnke, N. Neumann, O. Jagutzki, H. Schmidt-Böcking, R. Dörner, and I. Mančev, *Phys. Rev. A* **79**, 064701 (2009).
 - [10] O. Woitke, P. A. Závodszky, S. M. Ferguson, J. H. Houck, and J. A. Tanis, *Phys. Rev. A* **57**, 2692 (1998).
 - [11] J. L. Forest, J. A. Tanis, S. M. Ferguson, R. R. Haar, K. Lifrieri, and V. L. Plano, *Phys. Rev. A* **52**, 350 (1995).
 - [12] J. G. Murphy, K. F. Dunn, and H. B. Gilbody, *J. Phys. B* **27**, 3687 (1994).
 - [13] H. Atan, W. Steckelmacher, and M. W. Lucas, *J. Phys. B* **24**, 2559 (1991).
 - [14] R. D. DuBois, *Phys. Rev. A* **39**, 4440 (1989).
 - [15] P. Hvelplund and A. Andersen, *Phys. Scr.* **26**, 375 (1982).
 - [16] N. V. de Castro Faria, F. L. Freire, Jr., and A. G. de Pinho, *Phys. Rev. A* **37**, 280 (1988).

- [17] B. Peart, K. Rinn, and K. Dolder, *J. Phys. B* **16**, 2831 (1983).
- [18] F. Melchert, K. Rink, K. Rinn, E. Salzborn, and N. Grün, *J. Phys. B* **20**, L223 (1987).
- [19] R. E. Olson, A. Salop, R. A. Phaneuf, and F. W. Mayer, *Phys. Rev. A* **16**, 1867 (1977).
- [20] M. B. Shah, T. V. Goffe, and H. B. Gilbody, *J. Phys. B* **11**, L233 (1978).
- [21] M. B. Shah and H. B. Gilbody (private communication).
- [22] A. Itoh, M. Asari, and F. Fukuzawa, *J. Phys. Soc. Jpn.* **48**, 943 (1980).
- [23] L. I. Pivovarov, V. M. Tabuev, and M. T. Novikov, *Zh. Eksp. Teor. Fiz.* **41**, 26 (1961) [*Sov. Phys. JETP* **14**, 20 (1962)].
- [24] E. Ghanbari-Adivi and H. Ghavaminia, *Eur. Phys. J. D* **66**, 318 (2012).
- [25] M. Purkait, *Nucl. Instrum. Methods Phys. Res. Sect. B* **207**, 101 (2003).
- [26] M. Das, M. Purkait, and C. R. Mandal, *Phys. Rev. A* **57**, 3573 (1998).
- [27] A. Dhara, M. Purkait, S. Sounda, and C. R. Mandal, *Indian J. Phys.* **75B**, 85 (2001).
- [28] J. K. M. Eichler, A. Tsuji, and T. Ishihara, *Phys. Rev. A* **23**, 2833 (1981).
- [29] D. S. F. Crothers and N. T. Todd, *J. Phys. B* **13**, 2277 (1980).
- [30] Dž. Belkić, *Phys. Scr.* **43**, 561 (1991).
- [31] R. L. Becker and A. D. MacKellar, *J. Phys. B* **12**, L345 (1979).
- [32] L. Liu, D. Jakimovski, J. G. Wang, and R. K. Janev, *J. Phys. B* **43**, 144005 (2010).
- [33] M. Kimura, *J. Phys. B* **21**, L19 (1988).
- [34] R. E. Olson and A. Salop, *Phys. Rev. A* **16**, 531 (1977).
- [35] M. Das, M. Purkait, and C. R. Mandal, *Eur. Phys. J. D* **8**, 13 (2000).
- [36] S. Azizan, F. Shojaei, and R. Fathi, *J. Phys. B* **49**, 085201 (2016).
- [37] S. Azizan, F. Shojaei, and R. Fathi, *J. Phys. B* **49**, 135201 (2016).
- [38] S. Azizan, R. Fathi, and F. Shojaei, *Eur. Phys. J. D* **71**, 21 (2017).
- [39] E. Ghanbari-Adivi and H. Ghavaminia, *Chin. Phys. B* **24**, 033401 (2015).
- [40] R. Samanta, S. Jana, C. R. Mandal, and M. Purkait, *Phys. Rev. A* **85**, 032714 (2012).
- [41] I. Mančev, *Phys. Scr.* **51**, 762 (1995).
- [42] I. Mančev, *Phys. Rev. A* **54**, 423 (1996).
- [43] I. Mančev, *Phys. Rev. A* **75**, 052716 (2007).
- [44] I. Mančev, *Eur. Phys. J. D* **51**, 213 (2009).
- [45] Dž. Belkić, *Phys. Rev. A* **47**, 3824 (1993).
- [46] I. M. Cheshire, *Proc. Phys. Soc.* **84**, 89 (1964).
- [47] D. Dollard, *J. Math. Phys.* **5**, 729 (1964).
- [48] D. S. F. Crothers and L. Dubé, *Adv. At. Mol. Opt. Phys.* **30**, 287 (1993).
- [49] B. H. Bransden and M. R. C. McDowell, *Charge Exchange and the Theory of Ion-Atom Collisions* (Clarendon, Oxford, 1992).
- [50] A. K. Belyaev, A. Dalgarno, and R. McCarroll, *J. Chem. Phys.* **116**, 5395 (2002).
- [51] Dž. Belkić, *J. Phys. B* **26**, 497 (1993).
- [52] S. C. Mukherjee, K. Roy, and N. C. Sil, *Phys. Rev. A* **12**, 1719 (1975).
- [53] E. Clementi and C. Roetti, *At. Data Nucl. Data Tables* **14**, 177 (1974).
- [54] Dž. Belkić, *Phys. Rev. A* **37**, 55 (1988).
- [55] I. Mančev, N. Milojević, and Dž. Belkić, *Phys. Rev. A* **88**, 052706 (2013).
- [56] E. Ghanbari-Adivi and H. Ghavaminia, *Phys. Scr.* **89**, 105402 (2014).
- [57] E. Ghanbari-Adivi and H. Ghavaminia, *Few-Body Syst.* **55**, 1109 (2014).
- [58] S. K. Datta, D. S. F. Crothers, and R. McCarroll, *J. Phys. B* **23**, 479 (1990).
- [59] J. N. Silverman, O. Platas, and F. A. Matsen, *J. Chem. Phys.* **32**, 1402 (1960).
- [60] M. S. Schöffler, J. N. Titze, L. P. H. Schmidt, T. Jahnke, O. Jagutzki, H. Schmidt-Böcking, and R. Dörner, *Phys. Rev. A* **80**, 042702 (2009).
- [61] R. Gayet and J. Hanssen, *J. Phys. B* **25**, 825 (1992).
- [62] R. Gayet, J. Hanssen, and L. Jacqui, *J. Phys. B* **28**, 2193 (1995).
- [63] T. G. Winter and C. C. Lin, *Phys. Rev. A* **12**, 434 (1975).
- [64] A. Itoh, T. J. M. Zouros, D. Schneider, U. Stettner, W. Zeitz, and N. Stolterfoht, *J. Phys. B* **18**, 4581 (1985).